CNRS
Centre National de la Recherche Scientifique

INFN
Istituto Nazionale di Fisica Nucleare

Green Arm Cavity Length Noise Requirement

VIR-0461C-20

Jonathan Brooks[1*], Julia Casanueva[1], and Maddalena Mantovani[1]

[1] *EGO - European Gravitational Observatory*

Date: December 28, 2020

[*] *corresponding author:* brooks@ego-gw.it

VIRGO* A joint CNRS-INFN Project
Via E. Amaldi, I-56021 S. Stefano a Macerata - Cascina (Pisa)
Secretariat: Telephone (39) 050 752 521 * FAX (39) 050 752 550 * Email: ego@ego-gw.it

Contents

1 Introduction

The auxiliary lasers system (ALS) will be used in the lock acquisition of AdV+ to lock the arm cavities away from the infrared laser resonance while the center interferometer (CITF) is locked [4]. When designing the controller filter it is important to know the expected noise sources. For the green arm cavities, the primary noise sources are seismic disturbances [2] and frequency noise introduced by the optical fiber [3]. Further, the maximum allowable noise should be predicted in order to verify a proper safety margin for any unforeseen noise.

The green cavity lock is simulated in time-domain by using End-to-End software (e2e) [1]. By simulating the lock, preliminary locking strategies and controller filters may be tested. In Advanced Virgo (AdV), magnet-coil pair actuators reliably control low frequency noise (seismic noise), even up to earthquake level disturbances [5]. For Advanced Virgo Plus (AdV+), additional high frequency noise content is anticipated for the green cavity lock due to optical fiber noise. [3]. A frequency controller is included in the ALS and used in e2e to simulate the allowable noise, particularly at high frequencies.

In this note, the control system used in the e2e simulation is described in detail. Further, loop transfer functions from noise sources are developed. A filter for the maximum allowable noise is defined by applying performance requirements in the developed loop transfer functions. Finally, the results of a simulated lock acquisition using the maximum allowable noise filter are presented to verify the noise limit.

2 Theory

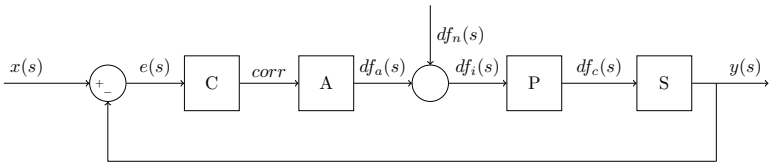

Figure 1: Block diagram for the arm cavity longitudinal control with frequency controller. Variables shown to define loop transfer functions, particularly noise coupling transfer functions.

The block diagram of the control system simulated with e2e is shown in Figure 1 with relevant variables labeled. The controlled variable is the laser frequency or cavity length. $y(s)$ is the actual laser frequency or cavity length. $x(s)$ is the set point; which in this case is the resonant frequency or length and is cyclic with the free spectral range. And $e(s)$ is the error defined as the $e(s) = x(s) - y(s)$. Frequency and length shifts are used interchangeably since they are simply related by the free spectral range,

$$\frac{d_f}{c/2L} = \frac{d_l}{\lambda/2}, \tag{2.1}$$

where, for the green cavity, the free spectral length is approximately 49,969 Hz or 266 nm. The $df_{(\,)}(s)$ symbols represent change in frequency, the control variable. $df_a(s)$ is the change in frequency due to the actuator, $df_n(s)$ is due to noise, $df_i(s)$ is the input change in frequency to the plant, and $df_c(s)$ is the frequency change transmitted by the plant. Finally, *corr* is the correction voltage sent to the actuator.

Note for ALS, the green light enters through the ETM, and therefore the reflection is of the ETM mirror.

2.1 Component Description

P, Plant Long arm cavity with green laser. Consists of a single pole determined by mirror parameters at $\lambda = 532$ nm. High frequency disturbances are damped by the cavity.

$$p_g = 128.8\,Hz \tag{2.2}$$

Input Frequency change [Hz]
Output Transmitted frequency change [Hz]

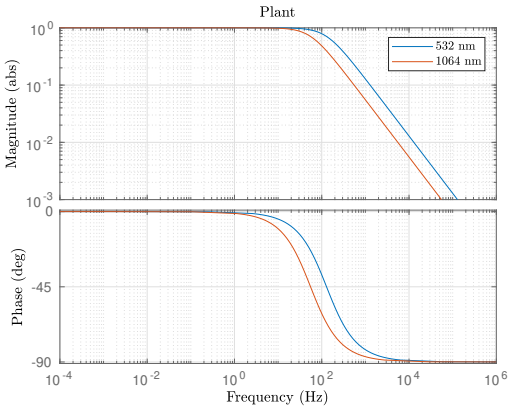

S, Sensor Normalized Pound Drever Hall (PDH) signal. For this note the PDH signal is the demodulated signal in reflection normalized by transmitted DC power. This component is simply a constant gain which is the slope of the PDH error signal. The slope of the error signal is the linear fit of the normalized error signal to the change in frequency into the arm cavity simulated by e2e for a free-swinging cavity. The figure to the right shows the calculation of the slope of the error signal. Only the data where the transmitted DC power was over 15% of the maximum transmitted DC power (shown in red) were used to calculate the fit.

Input Frequency change transmitted by cavity [Hz]
Output Normalized error signal [V/V]

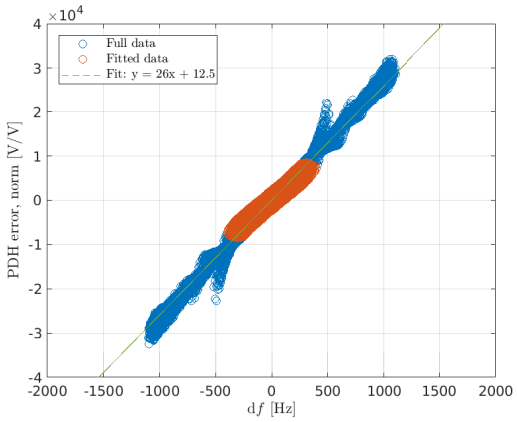

C, Controller Frequency actuator control filter. At this point, the filter is simply an integrator, a zero to cancel the plant pole and a gain calculated so that the open loop transfer function unity gain frequency is 10 kHz with a sampling frequency of >100 kHz.

Input Normalized error signal [V/V]
Output Correction signal to actuator [V]

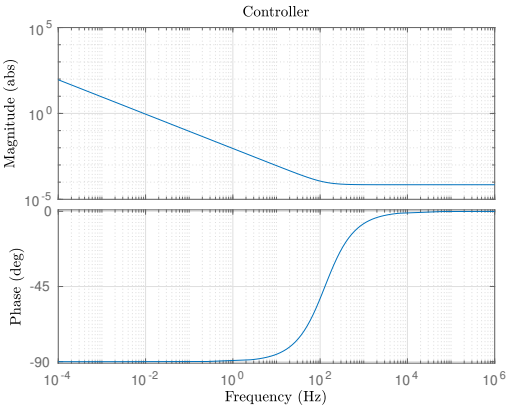

A, Actuator The frequency actuator consists of several components which change the gain and place pole frequencies. 1) a voltage control oscillator (VCO) with a gain of 4,000kHz/V and pole at 30 kHz, 2) A divider to reduce the gain to 23 kHz/V, 3) an acousto-optic modulator with a gain of 1 and a pole at 40 kHz, and 4) a second harmonic generator with a gain of 2 to convert the infrared to green. Note: in e2e the frequency is converted to a length changed enforced on the mirror to simulate a frequency shift.
Input Correction signal to actuator [V]
Output Frequency change inputted to cavity [Hz]

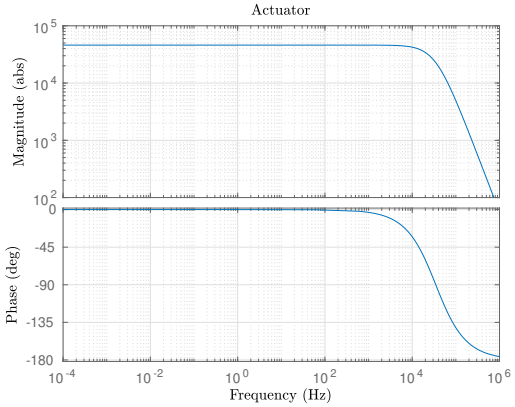

2.2 Loop Transfer Function

Several useful transfer functions may be derived from the component definitions and the block diagram shown in Figure 1. The most basic is the open loop transfer function (OLTF). This is simply a multiplication of all the components and is equivalent to removing the feedback loop in the bottom of Figure 1,

$$\begin{aligned} y(s) =& CAPSx(s) \\ OLTF = \frac{y(s)}{x(s)} =& CAPS. \end{aligned} \tag{2.3}$$

The open loop transfer function shows how an initial disturbance is operated on by the system. Figure 2a shows the Bode diagram of the OLTF. Note that the UGF is at 10kHz as designed.

The closed loop transfer function (CLTF) is also derived from Figure 1 by considering the feedback loop and the setpoint, $x(s)$. The set point for this system is the nearest resonance condition and is cyclic with the free spectral range. The system function for a the CLTF with no noise may be derived as

$$\begin{aligned} y(s) =& x(s) - CAPSy(s) \\ CLTF = \frac{y(s)}{x(s)} =& \frac{1}{1+CAPS} = \frac{1}{1+OLTF}. \end{aligned} \tag{2.4}$$

Figure 2b shows the CLTF response for the system. The plot shows that for low frequencies, any error in the system is reduced by many orders of magnitude, increasing as f until the UGF. Above the UGF the controller is noneffective and disturbances are transferred directly.

Another useful transfer function is from frequency change due to noise $df_n(s)$ to frequency change transmitted by the plant $df_c(s)$, which may be derived as

$$\begin{aligned} df_c(s) =& Pdfn(s) - CAPSy(s) \\ \frac{df_c(s)}{dfn(s)} =& \frac{P}{1+CAPS} = P * CLTF \end{aligned} \tag{2.5}$$

This transfer function describes how much noise is transmitted through the cavity under control.

Finally, the transfer function from frequency change due to noise $df_n(s)$ to correction voltage $corr$ is useful to determine the controller effort due to noise disturbances. This transfer function is defined as

$$\begin{aligned} corr(s) =& -PSCdfn(s) - APSCcorr(s) \\ \frac{corr(s)}{dfn(s)} =& \frac{-PSC}{1+APSC} = -PSC * CLTF. \end{aligned} \tag{2.6}$$

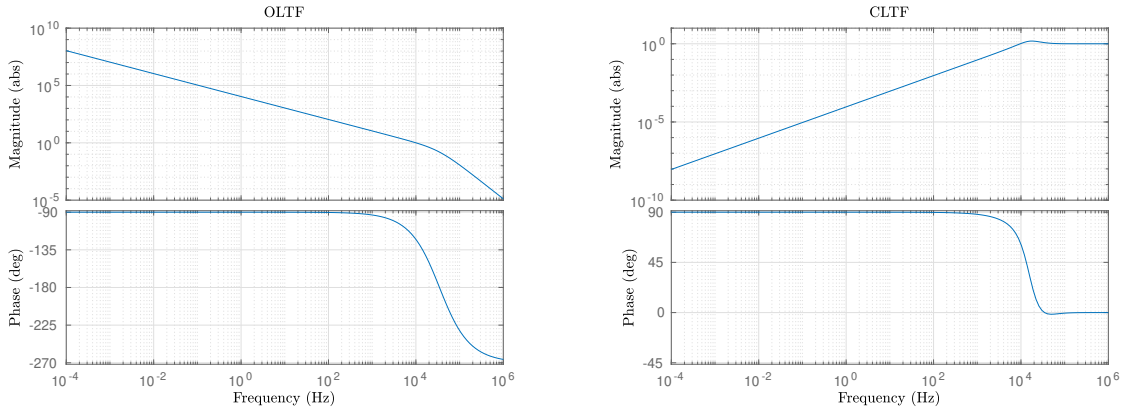

(a) OLTF (b) CLTF

Figure 2: Open and closed loop transfer functions. Note that the UGF is at 10kHz.

2.3 Maximum Allowable Noise

The maximum allowable noise allowed for the frequency controller is determined by three constraints:

1. **avoid actuator saturation** the frequency actuator saturates at 10V. The maximum allowable frequency noise is calculated by substituting 10 V for *corr* in Equation 2.6 and solving for $df_n(s)$.

2. **achieve control accuracy to maintain 99% of intracavity power** the transmitted DC power is used as a measurement of cavity power. In order to maintain 99% of the transmitted DC power, the cavity must be within 0.07 nm of the resonant length (according to the transmitted DC power vs. cavity length Gaussian). The maximum allowable noise is calculated by substituting 0.07 nm (as a frequency by using Equation 2.1) for $df_c(s)$ in Equation 2.5 and solving for $df_n(s)$.

3. **allow time power to build in cavity** the lock of the arm cavity is not attempted until the PDH error signal is in the linear region which is guaranteed when the transmitted DC power reaches 50% of the maximum power. The frequency noise must be low enough so that the cavity power has time to build to the 50% threshold, putting a limit on the cavity speed. The rise time was determined to be $t_r = 1.53ms$ by simulating a stationary cavity in e2e. So long as the cavity stays within the full width at half maximum ($fwhm = 257$ Hz) the power will build to at least 50% within the rise time. Since this requirement is a speed, the magnitude of the noise is dependent on the frequency. Therefore this constraint adds a integrator filter instead of a simple gain. Assuming that the cavity is moving at a constant velocity, the noise gain is the full width at half maximum multiplied by the sampling frequency (100 kHz) applied at a frequency of $1/t_r$. Because the simulation time step is equivalent to the ITF sensor sampling time, the noise limit is equivalent. The maximum allowable noise is calculated by dividing this filter by the transfer function in Equation 2.5.

Figure 3 plots the noise level constrains in the relevant frequency and magnitude range. The maximum allowable noise is calculated as the minimum of these curves. As shown, the maximum allowable noise is not governed by the 99% power accuracy. The filter is defined by using the third constraint transfer function as this dominates at high frequencies. This transfer function has a double pole at 0. The double poles at 0 is replaced by a double pole at the crossover frequency with the actuator saturation limit, 0.2 Hz. The allowable noise filter is then defined as

$$H_n(s) = \frac{6.9977e-14(s+809.4)^2(s+3.246e05)(s^2+1.153e05s+9.965e09)}{(s+1.257)^2(s+809.4)(s+1.885e05)(s+2.513e05)}. \tag{2.7}$$

Figure 3 hows that this filter accurately reproduces the minimum of all noise constraints. White noise with an amplitude of one was used as an input to the allowable noise limit filter in order to verify the correct definition

of the transfer function.

Also shown in Figure 3 are the noise magnitude from known sources: seismic disturbances and noise fluctuations due to the fiber optic. The ground noise is close to the allowable noise limit. However, this is not a concern as there is also the magnetic coil pair actuators (whose transfer function is not included in the plot) which can supplement the frequency actuator at low frequencies if needed. The frequency noise remains at least an order of magnitude below the allowable noise limit for all frequencies.

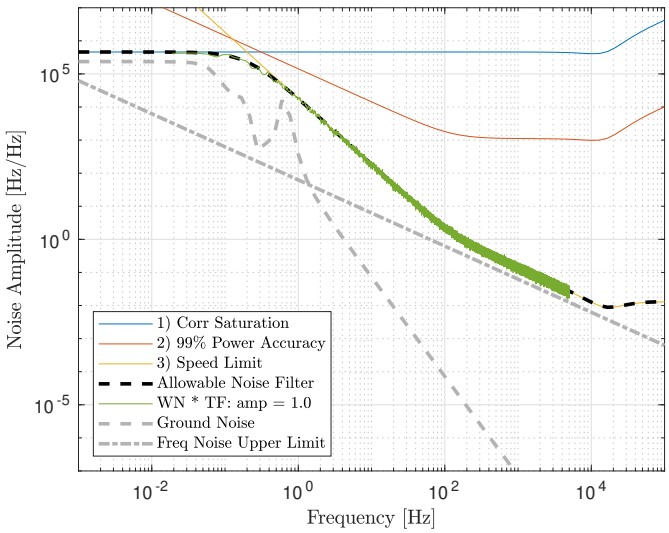

Figure 3: Maximum allowable noise filter defined as the minimum magnitude of anticipated constraining performance parameters. The filter is applied to white noise with an amplitude of one to show that the noise fluctuations remain below the maximum allowable curve. Also shown are the known ground and frequency noise levels.

3 e2e Lock Acquisition

The maximum allowable noise filter was verified by using e2e to perform a lock acquisition on the cavity. All noise sources were turned off except for the noise injection using the maximum allowable noise filter defined by Equation 2.7. Two simulations, long term/low resolution (20 min 100Hz) and short term/high resolution (1 min 100kHz), were performed in order to characterize the full frequency range. The noise amplitude was 1 for the 1 min simulation to verify that the high frequency noise was below the limit. This is the same which is used for the white noise in Figure 3. The 20 min simulation used a noise amplitude of 0.85 to ensure that fluctuations at low frequencies remained below the limit. Note, the amplitude is divided by $\sqrt{2}$ because e2e uses white noise such that the two-sided power spectral density (PSD) is equal to 1 whereas the filter was designed using a one-sided PSD.

Figure 4 shows the results of the simulation. The top left plot shows that the injected noise is just below the maximum allowable noise filter, as expected. The cavity was still able to lock with the higher noise amplitude of the 20 min simulation. As shown in the plot, the noise exceeds the noise filter at higher frequencies which may indicate that the maximum allowable noise filter is conservative. The top right plot shows that PSD difference of the noise and the actuator. The difference is relatively low for the entire frequency range showing that the actuator is accurately correcting the noise. The high resolution data matches the noise PSD except above the UGF where the difference increases as $1/f$. The bottom left plot shows that the achieved control accuracy is well above the required 99% based on the transmitted DC power. The 3σ value is within 0.1% of the maximum transmitted DC power. A stable distribution is fit to the data. The short term data shows a distribution which is nearly a normal distribution, $\alpha \approx 2, \beta \approx 0$. The long term data shows that the distribution is slightly

skewed negative, towards lower power. This is to be expected as the values above 1 are due to electrical noise in the photodiode, and the increased statistics negative can be attributed to the longer simulation. Finally, the bottom right plot shows that the correction voltage. For the short simulation, it is well below saturation. However, for the longer simulation there are some point above the saturation limit of the actuator. This may be attributed to the higher noise amplitude applied to the filter. In practice, the magnet coil actuators on the mirror may be used to supplement this low frequency drift. Further, the upper left plot shows that some of the noise measurements are above the noise limit curve.

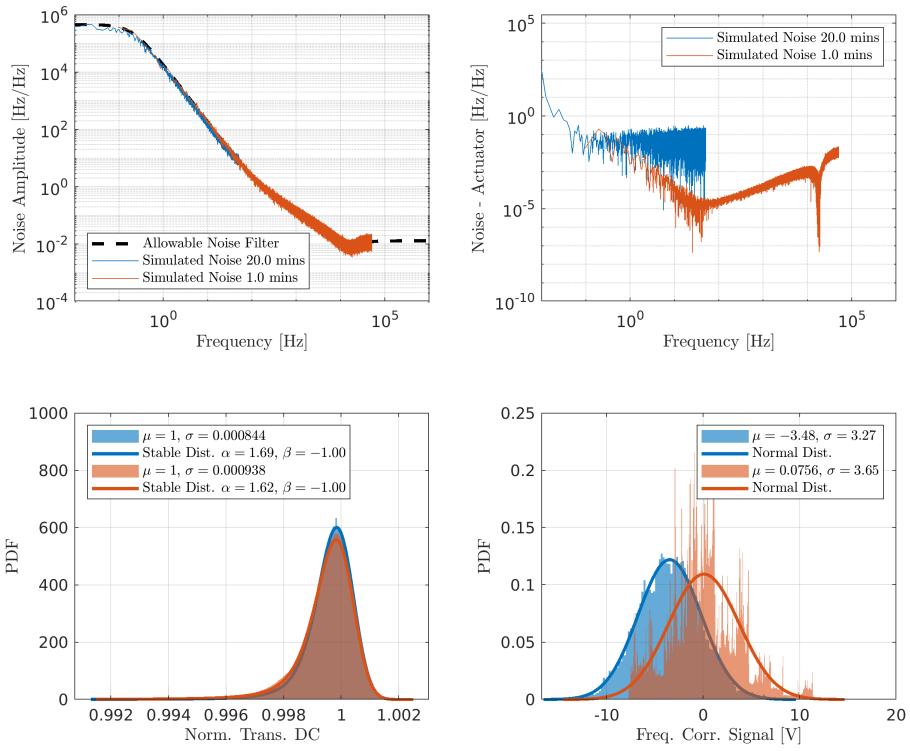

Figure 4: Performance of lock acquisition e2e simulation for long term/low resolution and short term/high resolution cases showing a successful lock with the maximum allowable noise filter applied. The lock accuracy was well within the requirement of 99% of the maximum transmitted DC power. The data beyond the actuator saturation limit may be mitigated by using the mirror magnet coil actuators.

Figures 5 and 6 show the time series plot of the cavity lock performance. The zoomed plots on the left show the lock acquisition which occurs around 2 seconds for each simulation, generally with a different y-axis scale. Figure 5 shows the high resolution simulation overlaid on the first minute of the long term simulation. During the lock acquistion several peaks occur in the normalized transmitted DC power which correspond to the cavity length passing through a resonance. The PDH signal correspondingly becomes linear during these peaks. The corrections are zero until the lock acquisition flag is set, at 2 seconds. Shortly following this, and on the next peak, the linear control closes and the cavity remains locked. The lock is again shown to be very accurate as the root mean square (RMS) of the cavity length frequency variation remains below 0.01% of the free spectral range (FSR). The corrections in closed loop indicate the amount of noise present in the cavity as corrections counteract the noise in order to keep the cavity length variations low. The RMS of the corrections are 4.47 FSR ($223kHz$, $1.18\mu m$) and 1.2 FSR ($60.0kHz$, $0.319\mu m$) for the long term and high resolution simulations, respectively. Figure 6 shows a longer timescale of the long term simulation only.

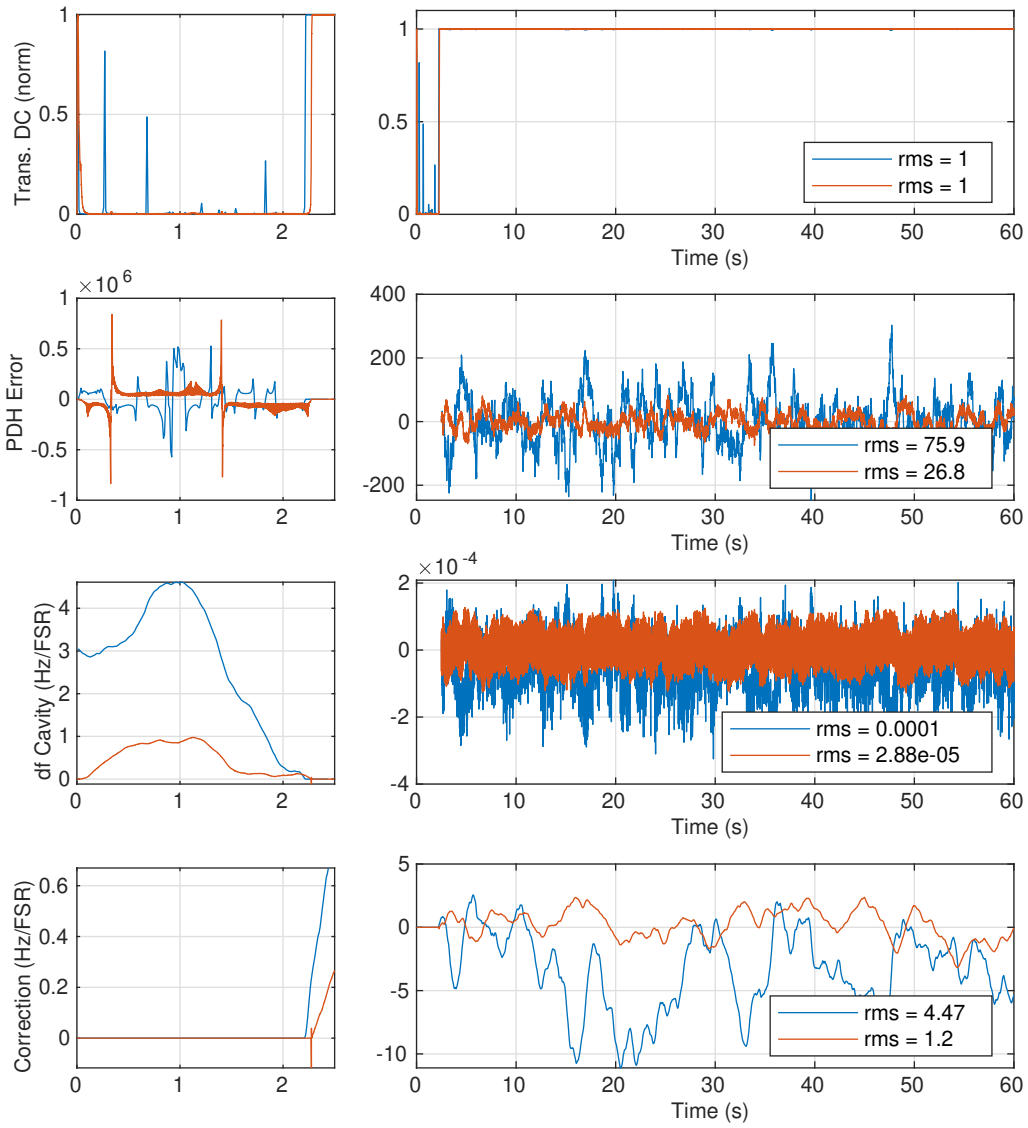

Figure 5: Time series of the cavity lock performance for the high resolution simulation overlaid on the first minute of the long term simulation. The lock acquisition is shown in the zoomed plots on the left showing proper behavior of the transmitted DC and PHD error signal as the cavity passes through resonances. The lock acquisition is enabled at 2 seconds. The lock is shown to be very accurate due to the low RMS values of the cavity length variation.

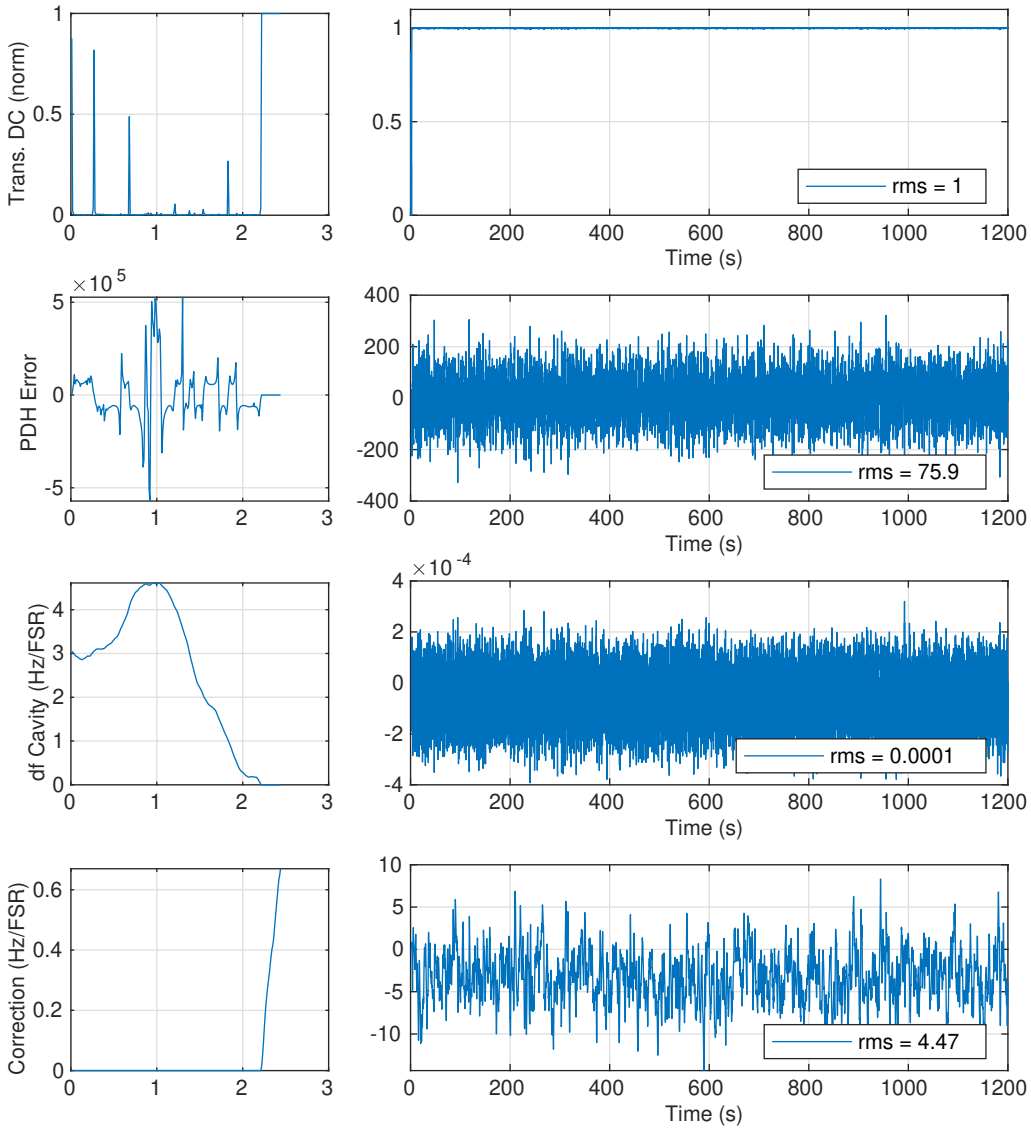

Figure 6: Time series of the cavity lock performance for the full timescale of the long term simulation.

4 Conclusion

The maximum allowable noise filter has been identified and defined by Equation 2.7. The cavity lock acquisition using the maximum injected noise has been verified by using e2e. The accuracy and correction voltage are within the required design values. The maximum allowable noise limit may be increased with a more complex control filter. However, the current level of noise is satisfactory below the maximum allowable limit.

5 Considerations for Future Work

During course of this investigation, the error signal hand-off from green to infrared was considered. After the CITF is locked, the frequency of the locked green cavity will slowly change so that the gap between the green and infrared resonances will converge. Casanueva and Leroy [3] showed by a FINESSE simulation that during this hand-off the infrared laser becomes resonant in when this gap is reduced to 7 Hz. This requirement was not included in the present analysis as it occurs after the green lock acquisition. However, this point should be revisited in the future.

The controller presented in this paper is a basic controller intended to be used as a baseline for development. The controller shows satisfactory performance in the present simulation. However, real-world applications may require additional development of the controller, e.g. a roll off at high frequency.

A Data and Filter Location

The following file locations are valid at the time of writing.

The slope of the PDH signal was calculated from the free swinging cavity located in the directory `/data/dev/optics/Simulation/e2e/greenCavity/02_freeSwingingMaxima`.

The maximum allowable filter defined in this note may be located in the file `/data/dev/optics/Simulation/e2e/greenCavity/allowableNoiseFilter.mat`.

The simulation data for the verification data may be located at `/data/dev/optics/Simulation/e2e/greenCavity/allowableNoise/`.

References

[1] Biplab Bhawal, Matt Evans, Ed Maros, Malik Rahman, and Hiro Yamamoto. Getting started with end-to-end model. *Internal Working Note of the LIGO Project*, LIGO-T980051-00-E, 1998. 2

[2] Jonathan Brooks, Julia Casanueva, and Maddalena Mantovani. Time domain simulation of the green cavity lock in advanced virgo +. *Virgo Note*, VIR-0527A-20, 2020. 2

[3] J. Casanueva and N. Leroy. Auxiliary laser system: study of the lock acquisition strategy. *Virgo Note*, VIR-0327A-19, 2019. 2, 10

[4] The Virgo Collaboration. Advanced virgo technical design report. *Virgo Note*, VIR-0128A-12:pp. 336–338, 2012. 2

[5] Paolo Ruggi. Lock in ln3 using ni/wi mar_z_corr instead of ne/we. Logbook entry 45661, VIRGO, 2019. https://logbook.virgo-gw.eu/virgo/?r=45661. 2